Received: 11 October 2021 | Revised: 7 December 2021 | Accepted: 12 January 2022

High Voltage

DOI: 10.1049/hve2.12200

ORIGINAL RESEARCH

Experimental verification of the potential of superhydrophobic surfaces in reducing audible noise on HVAC overhead line conductors

Xu Zhang[1] | Ian Cotton[1] | Qi Li[2] | Simon M. Rowland[1] | Christopher Emersic[1] | Chengxing Lian[1] | Wenyuan Li[1]

[1]Department of Electrical and Electronic Engineering, The University of Manchester, Manchester, UK

[2]School of Electrical Engineering, Chongqing University, Chongqing, China

Correspondence

Xu Zhang, Department of Electrical and Electronic Engineering, The University of Manchester, Oxford Rd, Manchester, UK.
Email: xu.zhang-10@postgrad.manchester.ac.uk

Associate Editor: Xingming Bian

Abstract

Overhead line conductors can generate audible noise across a wide frequency spectrum as a result of elevated electric fields at the conductor surface. Such fields are enhanced by the presence of surface defects, insects, water drops and pollution. Within this paper, the impact of a superhydrophobic coating on the audible noise produced by an overhead line conductor is examined. Noise levels from a conductor coated with a superhydrophobic coating were compared to those from a bare conductor in a semi-anechoic chamber. The conductors were energised at voltages to provide surface electric fields ranging from 6 kV/cm to 21 kV/cm (rms). With a continuous water spray system depositing droplets on the conductor surface, the frequency domain sound pressure level, overall sound pressure levels and corona discharge magnitude were measured. It is demonstrated that the use of a superhydrophobic coating reduced audible noise levels and corona discharge magnitude, especially at electric fields above 14 kV/cm. The image analysis suggests that the water drop size distribution and the position of surface droplets on the conductor circumference play an important role in the magnitude of audible noise.

1 | INTRODUCTION

There has been a continued growth in the use of ultra-high-voltage (UHV) and extra-high-voltage (EHV) overhead power lines to meet the increasing demand for electrical transmission capacity [1–3]. As energy systems transition to meet climate change targets, it is inevitable that new/upgraded overhead line infrastructure will be required. Overhead line conductors are designed to fulfil not only electrical and mechanical requirements but also to meet a number of environmental constraints, including maximum electric/magnetic fields, audible noise levels, corona loss and radio interference [4–8]. This paper is focussed on the issue of audible noise.

Audible noise is generated from an overhead line conductor when the surface electric field of the conductor exceeds a specific threshold. The risk of audible noise is increased by the presence of water droplets, insects, or pollution on the conductor that provides local enhancement of the electric field [9]. The audible noise emitted from AC transmission lines consists of two key components: a wide spectrum in the 1–20 kHz range that is heard as a high pitch, crackling noise, and a low-frequency hum at twice the power system frequency (100 or 120 Hz) [10–13]. The higher frequency crackling noise is primarily a result of corona discharge (an incomplete electrical discharge due to ionisation of the air surrounding a conductor [14]) developing at the location of protrusions on the conductor surface [15]. The low-frequency humming noise is usually a more significant concern as it can propagate over larger distances and through buildings and is a source of noise complaints from local residents [16, 17].

There have been a number of mechanisms suggested for the generation of the low-frequency hum. Straumann explored simulations of oscillating airborne ion distributions and calculations of sound pressure [18, 19]. It was concluded that ions were attracted and repelled from a conductor operating under an AC voltage and this movement caused pressure waves with

the twice frequency of the voltage. In contrast, Li et al. measured the time-domain waveforms of audible noise generated by a single corona source and correlated the audible noise pulses with corona current pulses happening simultaneously [20]. They describe how charged ions generated by the corona discharge are displaced in the air creating soundwaves of the power frequency and its harmonics [21]. Teich and Weber [22] simultaneously measured partial discharge current and audible noise and found that the 100 Hz noise was 35 dB even when the discharge was extinguished. As such, they showed that low-frequency noise would exist even without partial discharge. They observed the motion of water droplets on the conductor under 50 Hz AC voltage waveforms and that the deformation of these droplets is periodic with a frequency of 100 Hz, leading to the low-frequency hum. Further studies have examined the behaviour of water droplets under an AC field on a conductor and insulator surface [23, 24], again finding that the water droplets vibrate periodically with a frequency of double the applied voltage. Fujii et al. [25] analysed forces on droplets and concluded that the droplets deformed with double the excitation frequency under the Maxwell stress generated by the electric field.

Bian et al. [26] and Chen et al. [27] studied the relationship between audible noise and the surface roughness of a conductor. It was shown that roughness had a positive linear relationship with the level of audible noise. The interaction between the dielectrophoretic force and the particles caused by the extremely uneven electric field is the fundamental reason for the regular deposition of particles on the surface of the conductor, which promote the corona discharge and audible noise [28, 29]. Ianna et al. [30] studied the spectral properties of audible noise by a single corona source under AC voltage and found that audible noise increased linearly with applied voltage. Phase order and the choice of a compact line configuration also influence the surface electric field and noise level [31, 32]. Different conductor configurations have been shown to influence audible noise. A combination of an additional conductor in the centre phase and asymmetric bundles on all phases can be used to reduce audible noise levels [31]. Tanabe et al. [33] found that using a system that adds a sub-conductor to the bottom of regular symmetrical conductor bundles resulted in a reduced level of audible noise. Such improvements are ascribed to reduced electric fields at the location of water droplet accumulation along the underside of the lower conductors in the bundle. The corona discharge was also reduced with the decreasing surface gradient.

Surface treatments have previously been applied to conductors to examine their effects on audible noise. Paul [34] compared the noise performance of a hydrophobic conductor condensed with a paraffin film and a hydrophilic conductor prepared by heating it in an oven to 600°C. The results show that the hydrophobic conductor reduces noise level at low electric fields (around 11 kV/cm) and the hydrophilic conductor shows a reduction at 10–15 kV/cm. Miyajima and Tanabe [35] prepared conductors with hydrophobic painting, and sand and titanium blasting, giving a range of contact angles. The noise was reduced on hydrophilic and superhydrophobic conductor surfaces. Audible noise levels did not change significantly with the contact angle ranging from 0° to 90°. For a hydrophobic conductor with a contact angle greater than 90°, the audible noise level decreased as the contact angle increased. However, testing was not conducted in an anechoic chamber and low-frequency noise was not analysed.

In addition to noise reduction, superhydrophobic surfaces have shown potential in anti-icing and self-cleaning applications on insulators and transmission lines conductors [36]. However, the robustness of the superhydrophobic surface may be a limit for the application, and therefore, a research is also required on its longevity [37]. Previous research has included the durability of superhydrophobic coatings such as NeverWet® and laser micropatterned material [38, 39]. Thermal cycling up to 80°C over 1000 h and natural exposure to rain, snow, fog and contamination for 1 year have allowed some assessment of the longevity of these two surfaces. The contact angle and roll-off angle of the NeverWet® coating reduced from 165° to 162° and increased from 2.1° to 5.9°, respectively. The laser micropatterned samples did not show a reduction of the contact angle but saw a slight increase for the roll-off angle from 2.5° to 2.7°. After one year of natural exposure, the contact angle of coating and laser micropatterned samples reduced from 166° and 165° to 158° and 161°, respectively, and the roll-off angle increased to 10° and 6.5°. In summary: these two surfaces were degraded but maintained the superhydrophobicity after thermal and outdoor ageing.

Wang [40] developed a design of robust superhydrophobic surfaces through a combination of nanostructure and microstructure. The micro-surface-interconnected frames contain the pockets for placing the water-repellent nanostructure which provides the superhydrophobicity. This design aims to protect the nanostructure and provide durability. The samples suffering 1000 abrasion cycles and scratch tests maintain the superhydrophobicity and low roll-off angle less than 12°. This design may be applied to gain robust superhydrophobic surfaces.

In this study, we build on the work of Miyajima and Tanabe [33] and focus on assessing whether the use of a superhydrophobic coating on an overhead line conductor will decrease audible noise. Using a semi-anechoic chamber, an analysis of audible noise in the frequency domain—with a focus on low-frequency hum—is made for multiple types of conductors that are treated with a superhydrophobic coating. An assessment is thus made of the benefits that a superhydrophobic coated conductor could deliver in terms of noise reduction. The surface drop morphology was also analysed to examine its influence on audible noise. This work confirms the benefits of superhydrophobic conductors, enabling the design of environmentally improved compact overhead lines and increasing the voltage capability of existing installations. The work therefore justifies the further development activity required to translate this technology into practice.

2 | EXPERIMENTAL METHODOLOGY

2.1 | Anechoic chamber and sound measurement

A semi-anechoic chamber with dimensions 10.5 × 4.3 × 3.0 m (Figure 1) was constructed to minimise background noise and maximise the quality and accuracy of sound measurements. This consists of a 50 mm core of cross-layered mineral wool and an outer shell of 0.7-mm sheet metal. Internal sound wedges are made of porous foam and oriented to maximise sound absorption (Figure 1b) [41].

A noise analysis system from Brüel & Kjær included a BK Type 4961 multi-field microphone and acoustic software (Pulse). Ambient background noise measurements inside and outside the chamber confirmed the anechoic chamber reduces sound pressure level at all frequencies, with a 17 dB reduction at 100 Hz, and 25 dBA reductions in A-weighted overall sound pressure level.

2.2 | Samples

Test samples were 4 m lengths of traditional ACSR (Aluminium Conductor Steel Reinforced) conductor and GZTACSR (Gap Type Super Thermal-resistant ACSR) conductors, both with diameters of 31.6 mm (Figure 2). These are referred to as ACSR and GAP, respectively, in the remainder of this paper.

The commercial coating, NeverWet®, was evenly applied to the conductor surface to achieve superhydrophobicity. While this coating may not be suitably resilient to use in a real-world application, it nevertheless provided a rapid and repeatable way of generating a superhydrophobic surface in this study. Prior to the coating, acetone was used to clean the conductor surface and left to dry overnight. Three layers of NeverWet® were sprayed onto the conductor, the second one 15 min after the first, and the topcoat after waiting a further 30 min. Each layer of NeverWet® was sprayed on one side of the conductor for a total of 60 s (2 times × 30 s). Then rotate the conductor 90° and spray for 60 s. Repeat this process two more times, spraying the same amount of coating on the conductor. Coated conductors were allowed to dry overnight. The surfaces of the conductors before and after the superhydrophobic coating are shown in Figure 2. It shows the visual impact of the superhydrophobic coating on the GAP and ACSR conductor.

Water drops with a range of sizes were retained on the uncoated conductor primarily near the gaps between strands, in contrast to the coated sample which had very few. Quantifying static contact angles on a curved surface is difficult. Thus, flat samples made of aluminium alloy 6082 (a typical overhead line conductor material) were prepared with the superhydrophobic coating in the same way as the round conductors. The static contact angle was measured using a DataPhysics OCA 15EC goniometer. 5 μL drops of deionised water were placed on the uncoated and coated flat samples (Figure 3). The average static contact angle of the coated samples was measured to be 162.4°. The uncoated sample showed a contact angle of 85.3°. Materials giving angles above 150° are classified as superhydrophobic.

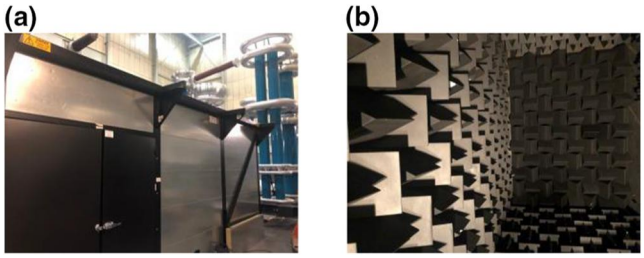

FIGURE 1 External and internal view of the anechoic chamber. (a) Overview of the anechoic chamber, (b) inside of the anechoic chamber

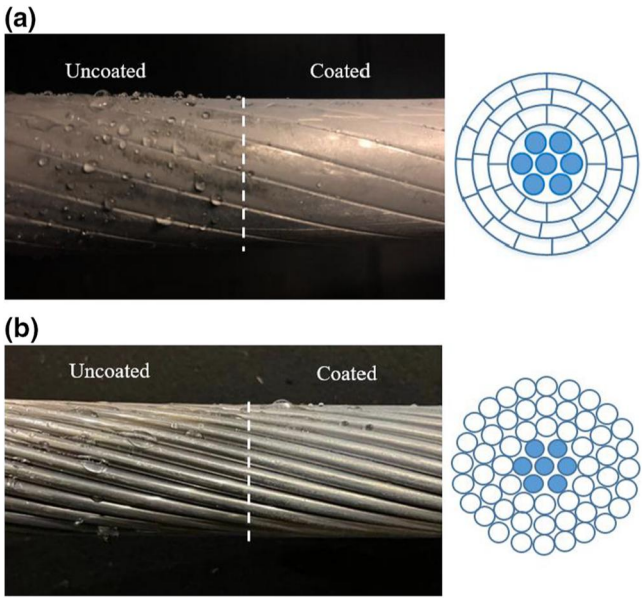

FIGURE 2 Images of water drops on uncoated and coated 31.6 mm diameter GAP and ACSR conductors together with the cross-section view. (a) GAP, (b) ACSR

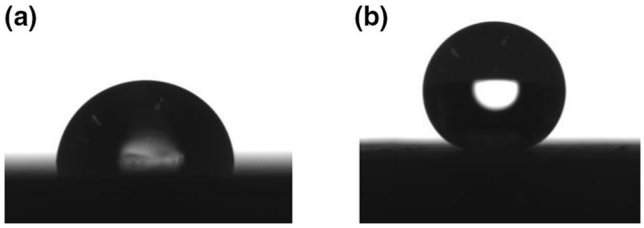

FIGURE 3 Goniometric microscopy images of a 5 μL water drop on a coated and uncoated flat metallic surface used to measure static contact angles. (a) Uncoated flat sample, (b) coated flat sample

2.3 | High voltage experimental setup

Figure 4 shows the experimental setup. An earthed cylindrical cage of 75 cm radius controls the surface electric field, ensuring 18 kV/cm (rms) when using a 110 kV (rms) 50 Hz power

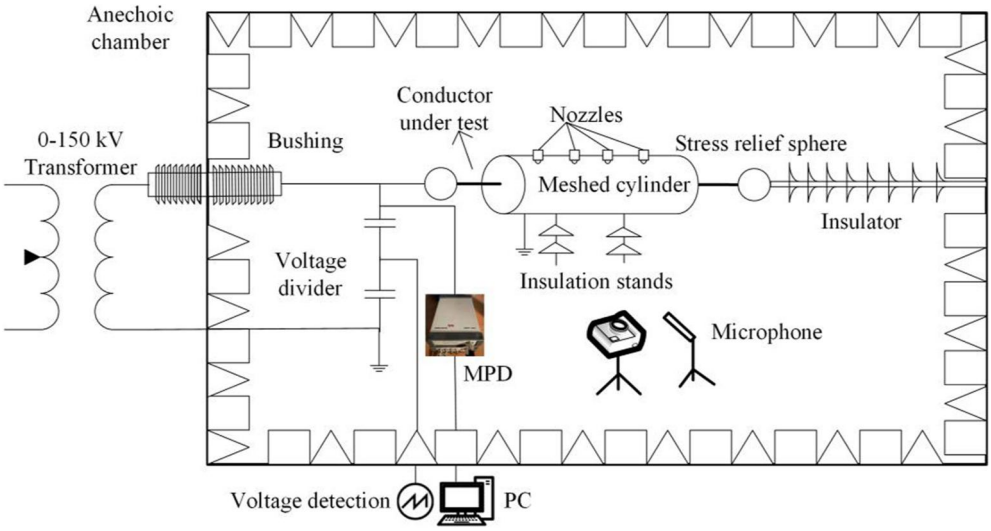

FIGURE 4 Schematic of an experimental setup. The semi-anechoic chamber has internal dimensions of 10.5 × 4.3 × 3.0 m. The cable under tests is 4 m long

supply [41]. This is equivalent to the average field strength seen on a 400 kV (rms) system twin bundle RUBUS conductor and effectively tests 4 m of the cable due to the limit of chamber size [42]. All the voltage and electric field values in the following are given as rms values. A bushing connects the cable sample to a 150 kV transformer through the wall of the anechoic chamber, with spheres placed at the end of the conductor under test to reduce the electric field and avoid end effects and associated localised discharges. It is critical that the transformer is external to the chamber to avoid low-frequency acoustic noise. The voltage was adjusted to supply the desired electric field at the surface of the conductor (determined by calculation) [42]. The high voltage is applied to the inner conductor while the outer meshed cage is earthed. This arrangement can increase the surface electric field by the presence of the cage and ensures the electric field is consistent and uniform around the whole conductor. The electric field was varied from 6 kV/cm to 21 kV/cm. The Omicron MPD Partial Discharge Analysis System is employed to test and analyse the corona discharge behaviour meanwhile the noise is measured.

To evaluate noise performance under rain conditions, Unispray Mark 1 adjustable water supply nozzles connected to a regulator were used to spray tap water, with a measured conductivity of 108.1 μS/cm, at 20 mm/h (which meets the wet test standard in IEC 60060-1 [43]). The rate was adjusted by varying the water pressure and the precipitation rate was measured by a standard rain gauge.

3 | RESULTS AND ANALYSIS

3.1 | Influence of water presence on noise levels

Table 1 shows the 100 Hz, 200 Hz and A-weighted frequency-averaged overall sound pressure level measurements over a period of 60 s produced by both uncoated and coated conductor types when dry and wet, with a surface electric field strength of 18 kV/cm. This data illustrates the influence of water on a conductor surface on noise output. For these measurements reported in Table 1, samples were pre-wetted and the spray was disabled during noise measurements to capture only the sound produced by drops from electrically driven processes. Background noise was measured in the absence of an electric field and without the spray system active.

The measurements confirm that wet conductors generate a significantly higher and steady level of both 100 Hz, 200 Hz and A-weighted noise, relative to dry conditions, as expected. It suggests that water droplets on the conductor are the reason for noise generation. The ambient noise level at 100 Hz is higher than 200 Hz because the low-frequency noise with the longer wavelength can be propagated easier and further than high-frequency noise [44]. Dry conditions also increased A-weighted overall sound pressure level and 200 Hz noise level above the background—likely because of small surface defects like scratches on the conductor causing corona discharge. The corona discharge was found to increase the noise levels above 100 Hz. It can also be found by comparing the uncoated and coated conductors' noise that the coating has a negligible influence on noise levels in dry conditions but reduces noise on wet conductors.

Figure 5 shows the frequency spectrum of sound generated above background as a function of the average electric field at the surface, using a fast Fourier transform of the time-domain data. These samples are uncoated and are subjected to continuous water spray, unlike the measurements described in Table 1. Background noise levels were measured accordingly, with the spray active in the absence of an electric field. Above 10 kV/cm, the sound intensity at 100 Hz shows a marked increase for both conductor types, with harmonics at 200 Hz [21, 41]. For GAP conductor, there is a noise level peak at 150 Hz, but not for the ACSR conductor. It was observed by

TABLE 1 Measured sound pressure levels (with standard deviations shown) of dry and wet uncoated and coated conductors

	Background	Dry	Wet	Background	Dry	Wet
	Uncoated GAP			**Uncoated ACSR**		
100 Hz (dB)	24.7 ± 6.3	25.1 ± 4.2	52.6 ± 0.2	26.1 ± 5.9	29.1 ± 3.4	48.9 ± 0.4
200 Hz (dB)	6.0 ± 5.4	27.6 ± 0.6	55.3 ± 0.2	8.4 ± 6.8	8.6 ± 5.7	54.6 ± 0.2
A-weighted overall SPL (dBA)	22.9 ± 1.1	29.6 ± 3.2	57.9 ± 0.3	23.4 ± 1.5	30.7 ± 0.2	59.1 ± 0.2
	Coated GAP			**Coated ACSR**		
100 Hz (dB)	25.2 ± 4.8	26.2 ± 4.5	49.4 ± 0.4	25.9 ± 6.2	30.8 ± 5.4	46.7 ± 0.3
200 Hz (dB)	7.2 ± 5.2	8.9 ± 2.6	53.6 ± 0.2	8.8 ± 5.9	9.4 ± 4.9	51.1 ± 0.2
A-weighted overall SPL (dBA)	22.1 ± 0.6	30.2 ± 3.5	56.2 ± 0.3	24.1 ± 1.3	31.2 ± 0.3	56.9 ± 0.3

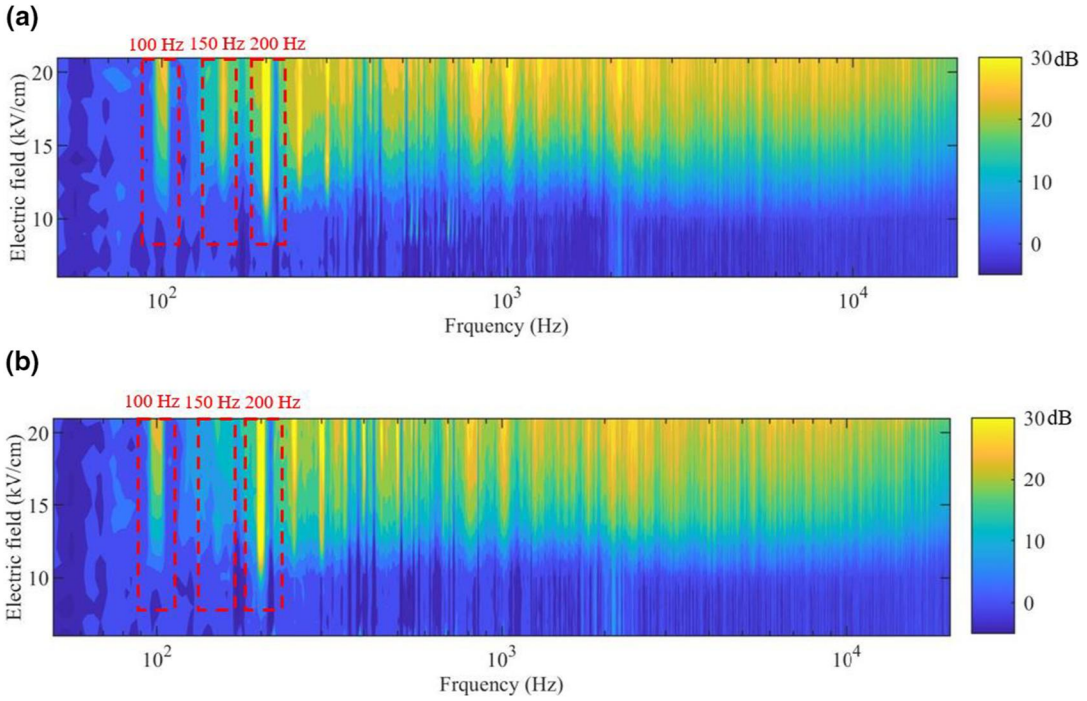

FIGURE 5 Measured noise levels (dB above background) as a function of electric field and frequency with continuous water spray on uncoated conductors. The 100 Hz, 150 and 200 Hz signals are highlighted by the red boxes, and units of the numerical levels associated with colours, given on the right, are in dB. (a) Uncoated GAP, (b) uncoated ACSR

our previous tests that some droplets on the uncoated GAP conductor vibrate at 150 Hz but not on the ACSR conductor [42]. High-frequency noise levels are also increased due to corona discharge. The 100 Hz noise levels of uncoated GAP and ACSR conductors increase to 59.3 and 53.4 dB, respectively, at the highest applied field, higher than the high-frequency noise levels.

3.2 | Influence of a superhydrophobic coating on noise levels

To understand the acoustic influence of the superhydrophobic coating, similar measurements were made on coated samples and the frequency spectrum of noise levels compared with uncoated samples. The differences with the results of Figure 5 are plotted in Figure 6. Noise level reductions compared to the uncoated conductors are mainly seen at low frequencies (below 1000 Hz) for both coated conductors compared with high-frequency noise (above 1000 Hz). For the GAP conductor, the main noise reduction is at 150 Hz and there are also reductions at 100 and 200 Hz. For ACSR conductor, there is a noise reduction at 100 and 150 Hz and the main reduction is around 200 Hz.

To gain a better understanding of audible noise reductions, the average of 100 Hz, low frequency (below 1000 Hz) and high frequency (above 1000 Hz), and A-weighted sound pressure levels of two repeated tests are shown in Figure 7. The 90% confidence intervals are included where possible, but the value is too small to distinguish at high electric fields. At

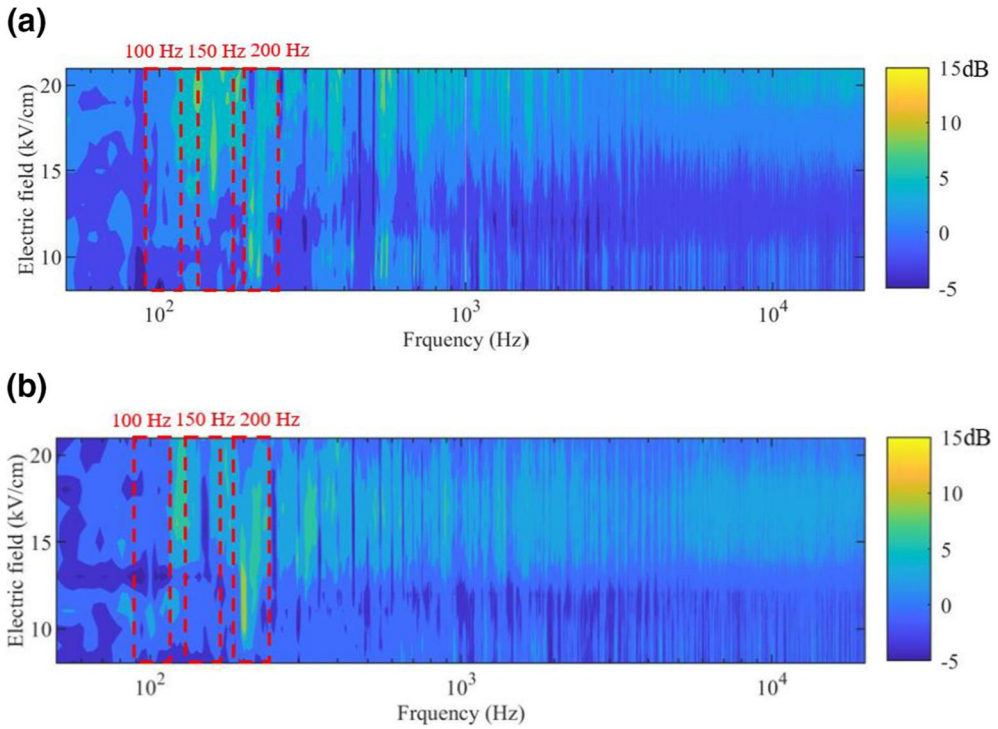

FIGURE 6 Measured noise levels reductions as a function of electric field and frequency with continuous water spray on uncoated conductors. The 100 Hz, 150 and 200 Hz signals are highlighted by the red boxes, and units of the numerical levels associated with colours, given on the right, are in dB. (a) The noise level reduction of coated GAP, (b) The noise level reduction of coated ACSR

electric field strengths below 10 kV/cm, low noise levels are produced mostly from the sprayer and the water impacting on conductors. Superhydrophobic coatings do not significantly reduce noise levels below this electric field strength. Above 10 kV/cm, the 100 Hz sound pressure level of uncoated and coated conductors increases, but less so for the coated conductors. A reduction in the noise level is seen on coated conductors at 11 kV/cm—this is examined further in Section 3.3 and the Discussion. Low-frequency noise levels are higher than that at the high frequency and superhydrophobic coating results in better acoustic performance for both conductors. Furthermore, A-weighted overall sound pressure levels do not show much difference below 14 kV/cm and as the electric field increases, coated conductors express lower noise levels compared with uncoated samples, showing the role of the superhydrophobic coating in reducing audible noise.

To further evaluate the noise level reductions with using the superhydrophobic coating at 18 kV/cm, the total sound power output from the conductor calculated by the overall sound pressure level, and the perceived loudness is given in Table 2. Sound power represents the acoustic power radiated by the sound source and can be calculated using equation (1) giving the overall sound pressure level (ISO 80000-8 [45]):

$$L_{\text{overall}} = L_{\text{I}} = 10\lg\left(\frac{I}{I_0}\right) = 10\,\lg\left(\frac{W}{W_0}\right) \tag{1}$$

where L_{overall} is the overall sound pressure level, L_{I} is the sound intensity level, I is the sound intensity, I_0 is the reference sound intensity, W is the sound power and W_0 is the reference (minimum audible) sound power (10^{-12} W). The sound power reduction is shown in equation (2):

$$\Delta W = 1 - \frac{1}{10^{\frac{\Delta L_{\text{overall}}}{10}}} \tag{2}$$

where ΔW is the sound power reduction and $\Delta L_{\text{overall}}$ is the overall sound pressure level reduction.

The psychoacoustic, perceived loudness depends on sound pressure level, the frequency spectrum, and the temporal delivery of the sound [46]. This is the quantity best suited to understanding how a human perceives the level of noise. The loudness reduction can be calculated using equation (3):

$$\Delta Z = 1 - \frac{1}{2^{\frac{\Delta L_{\text{p}}}{10}}} \tag{3}$$

where ΔZ is the loudness level reduction and ΔL_{p} is the sound pressure level reduction.

The measurements in Table 2 summarise the 100 Hz data and the calculated perceived loudness and sound power. They both show a perceived loudness reduction at 100 Hz, and low and high frequency as a result of the coating. The loudness reduction at the low frequency is greater than the reduction at the high frequency for both conductors. The sound power also shows a decrease after the superhydrophobic coating. All the noise reductions from the coating are greater for GAP than for ACSR, except at high frequencies.

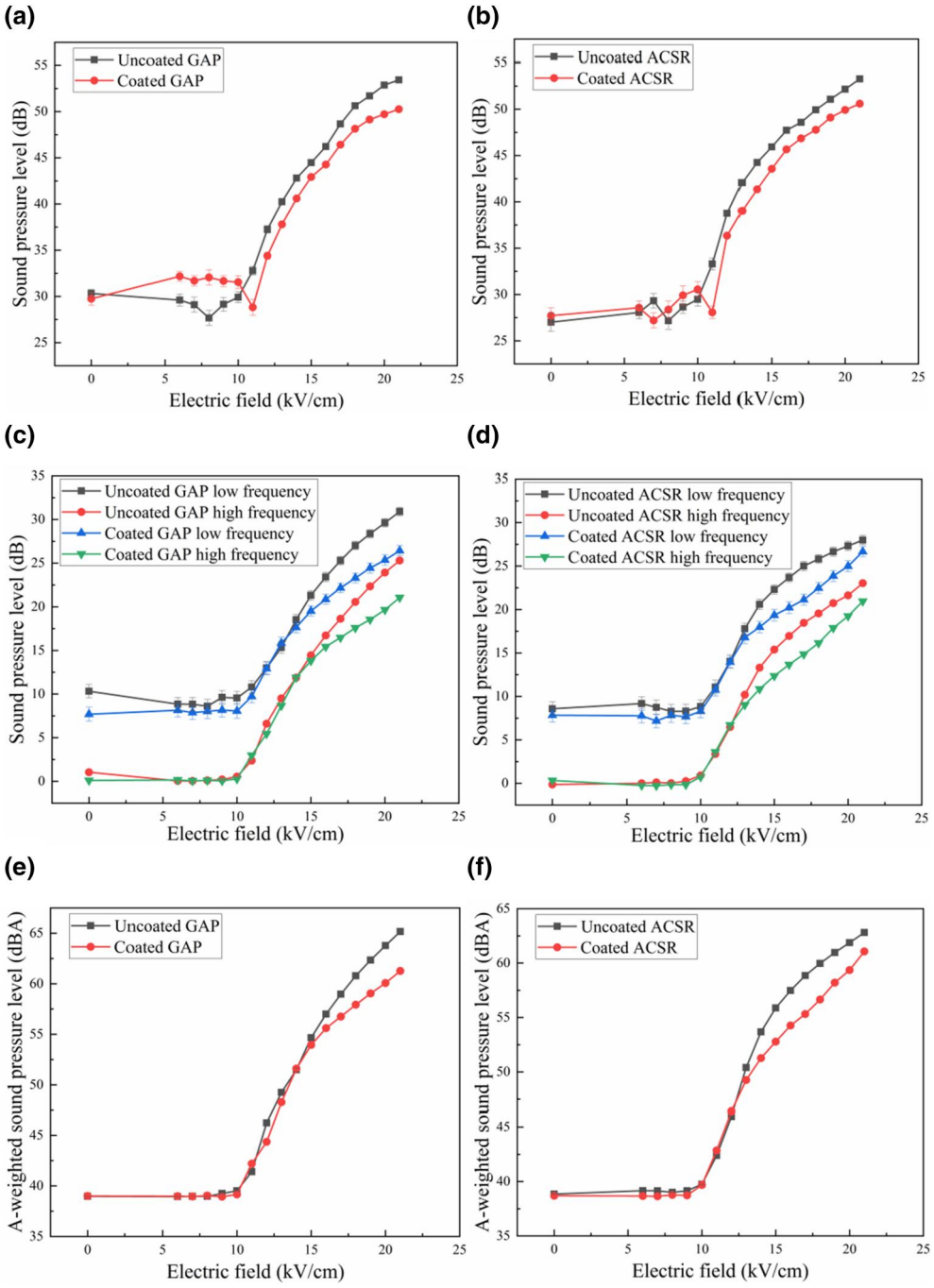

FIGURE 7 100 Hz, low and high frequency, and A-weighted sound pressure levels of uncoated and coated conductors with 90% confidence intervals. (a) (b) 100 Hz, (c) (d) low and high frequency, (e) (f) A-weighted sound pressure level

3.3 | Influence of drop morphology on sound output

Measurements have shown the superhydrophobic coating on the conductor reduces noise levels increasingly with higher electric fields. To explain this, the droplet morphology on the uncoated and coated conductors both without an electric field and with a field strength of 21 kV/cm is observed and compared in Figure 8.

On uncoated conductor samples, drops hanging on the underside of the cable deform with the changing electric field, oscillating between conical and flattened hemispheres [23]. Figure 8a–d shows that on uncoated samples, drops tend to hang from the bottom of the GAP conductor, with a few drops on the upper portion. Drops are more widely distributed on the circumference of the ACSR conductor. For coated samples (Figure 8e–h), drops become caught on the upward-facing flat strands of coated GAP conductor and trapped in

TABLE 2 Reduction in audible noise levels through application of coating

	SPL at 100 Hz (dB)	Reduction in perceived loudness (100 Hz)	Low frequency SPL (dB)	Reduction in perceived loudness (low frequency)	High frequency SPL (dB)	Reduction in perceived loudness (high frequency)	Overall SPL (dB)	Sound power(W)	Reduction in sound power
Uncoated GAP	50.63	15.85%	27.01	22.73%	20.56	18.61%	63.23	2.10×10^{-6}	44.02%
Coated GAP	48.14		23.29		17.59		60.71	1.18×10^{-6}	
Uncoated ACSR	49.93	13.85%	25.81	20.67%	19.55	21.05%	62.38	1.73×10^{-6}	33.47%
Coated ACSR	47.78		22.47		16.14		60.61	1.15×10^{-6}	

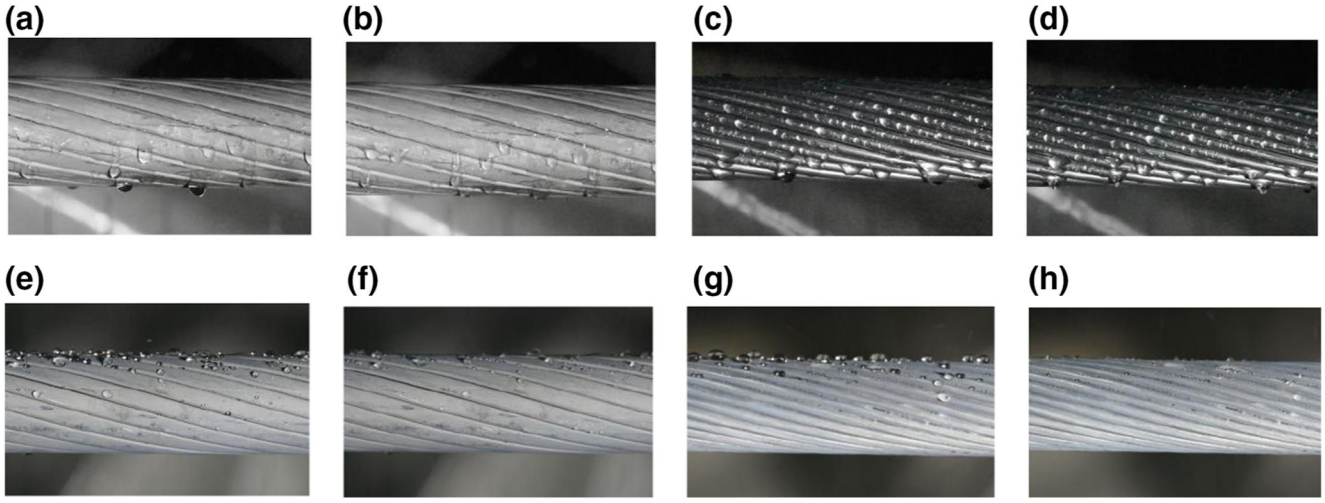

FIGURE 8 Images showing physical drop distribution on conductors with continuous water spray with and without a high field (E = 21 kV/cm) applied. (a) Uncoated GAP no E, (b) uncoated GAP 21 kV/cm, (c) uncoated ACSR no E, (d) uncoated ACSR 21 kV/cm, (e) coated GAP no E, (f) coated GAP 21 kV/cm, (g) coated ACSR no E, (h) coated ACSR 21 kV/cm

the grooves (interstices) on the upper surfaces of coated ACSR conductors, despite being superhydrophobic—particularly for ACSR conductors with more pronounced curvature in the strand geometry. Droplets on the lower sections of the conductor are rapidly repelled and fall from the superhydrophobic surface.

Below an electric field strength of 10 kV/cm, precipitation results in increasing droplet sizes on the coated conductor surface. Above 10 kV/cm, the high electric field and large contact angle of the droplets result in their bouncing and vibration and smaller droplet ejection from their surface, as imaged in Figure 9 [42]. The vibration process of a single droplet on the upward-facing surface of the uncoated conductor is shown in Figure 10. It can be seen that the vibration frequency is 100 Hz, twice the applied voltage frequency [23]. The electric force induced by the AC electric field stretches and retracts the droplet due to the surface tension and gravity [47]. When the electric force exceeds the surface tension and gravity, the tiny droplets will be ejected off the main part of a droplet.

Surface drop size distributions were quantified from the diameters of droplets measured in images for each experiment at an electric field strength of 21 kV/cm and compared with the corresponding 100 Hz, A-weighted overall sound pressure levels, low- and high-frequency sound pressure levels (Figure 11). In this article, the droplets were counted from four pictures consisting of two pictures captured during each test. The pictures were captured at the same position for each test from a vertical direction. Then, the diameter of the water drops can be measured by the image analysis software (ImageJ).

In Figure 11a, the black square represents the mean droplet diameter, the whiskers represent the associated standard deviation, the blue circles on the top represent a number of droplets on the conductors (the actual number over a 21 cm length are given) and the grey, red, blue and green bars give the A-weighted overall sound pressure level, 100 Hz, low- and high-frequency noise levels, respectively. From this, we see that the mean diameter of droplets on the coated GAP conductor is lower than on the uncoated one. However, the number of the droplets on the coated GAP conductor is higher than the uncoated one because most tiny droplets are trapped in the strands. Correspondingly, all the noise levels show a similar trend with droplet size.

Compared with the GAP conductor, more droplets are present on the ACSR conductor because of the round strands. Most small droplets are trapped in the grooves of the uncoated ACSR conductor, as shown in Figure 8. Several big drops are hanging on the bottom of the uncoated conductor, resulting in more droplets and a higher diameter of droplets.

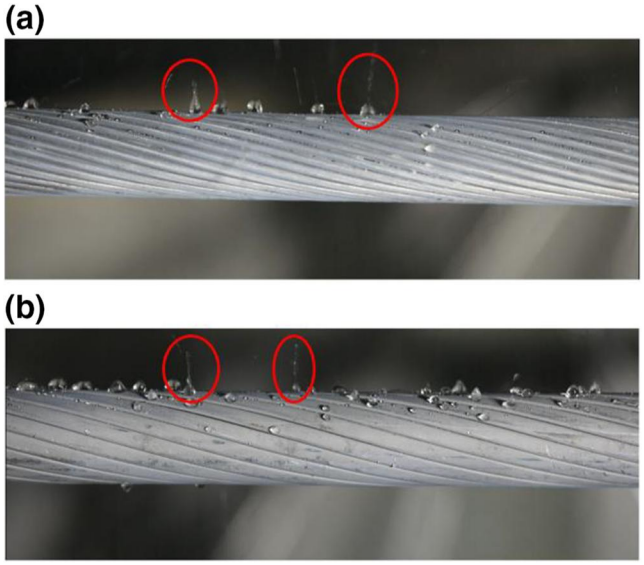

FIGURE 9 Drop vibration and droplet ejection on coated conductors at 11 kV/cm. Sessile droplets emitting smaller droplets are circled in red. (a) Coated ACSR, (b) coated GAP

The coated ACSR conductor shows lower sound pressure levels corresponding to droplets size. As the droplet size on the coated ACSR decreases, all the noise levels decrease. To gain a better understanding of droplet distribution, the droplet size histograms are shown in Figure 11b–e. The droplets on uncoated GAP are quasi-normally distributed but for coated GAP most droplet diameters are below 1.5 mm, which results in the lower mean diameter. The droplets on uncoated ACSR are mainly distributed all around the conductor circumference with similar size, showing that almost 90% of droplet diameters are below 2 mm. There are a few large pendant drops on uncoated ACSR contributing to a bigger mean diameter.

3.4 | Influence of corona discharge on sound output

The corona discharge inception voltage of the uncoated and coated conductors with continuous water spray was measured three times. The average corona inception voltages of uncoated and coated GAP were 37 and 46 kV, respectively. The uncoated ACSR and coated ACSR corona discharge inception voltage were 37 and 47 kV, respectively. Corresponding to the drop size distribution, the fewer and smaller droplets may result in higher corona discharge inception voltages. The corona discharge was observed by OFIL's DayCor Superb Ultraviolet camera, shown in Figure 12. The white dots represent photons generated by corona discharge. It is confirmed that corona discharge occurs near the tip of the water droplets.

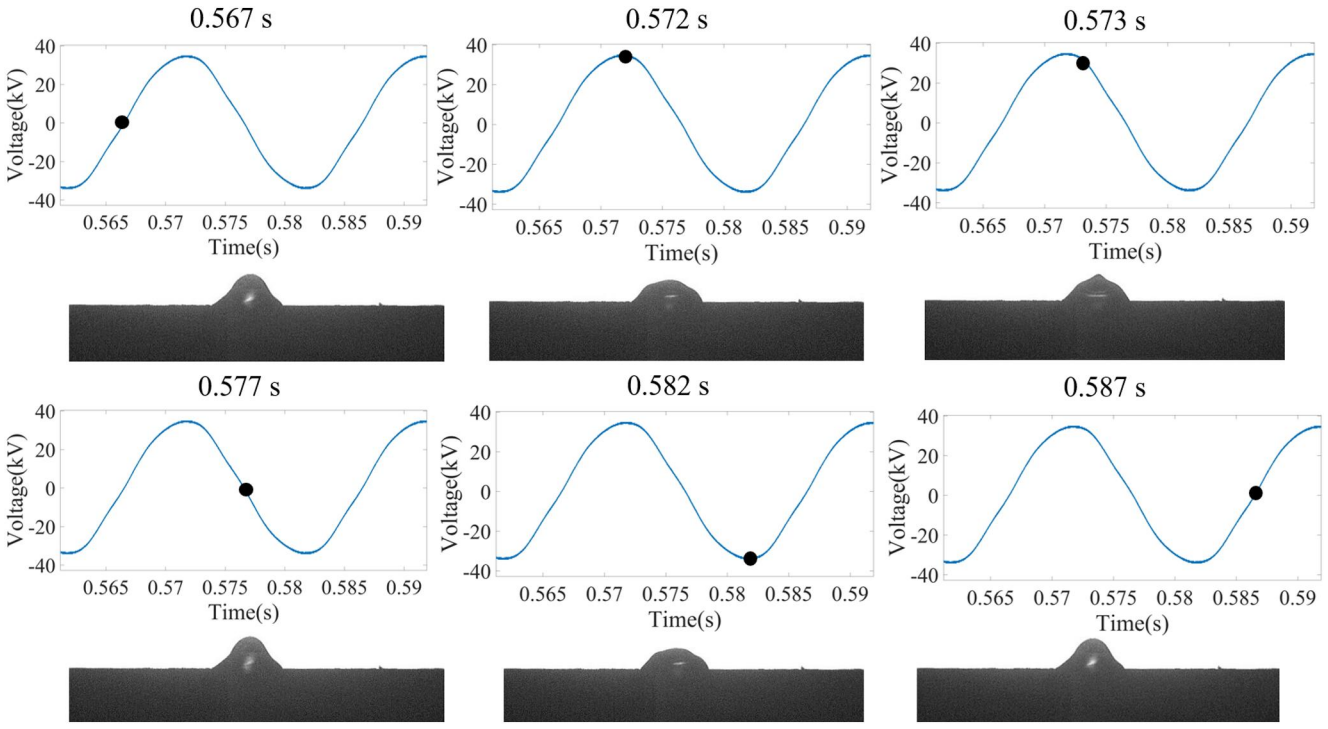

FIGURE 10 The droplet vibration process with synchronous voltage

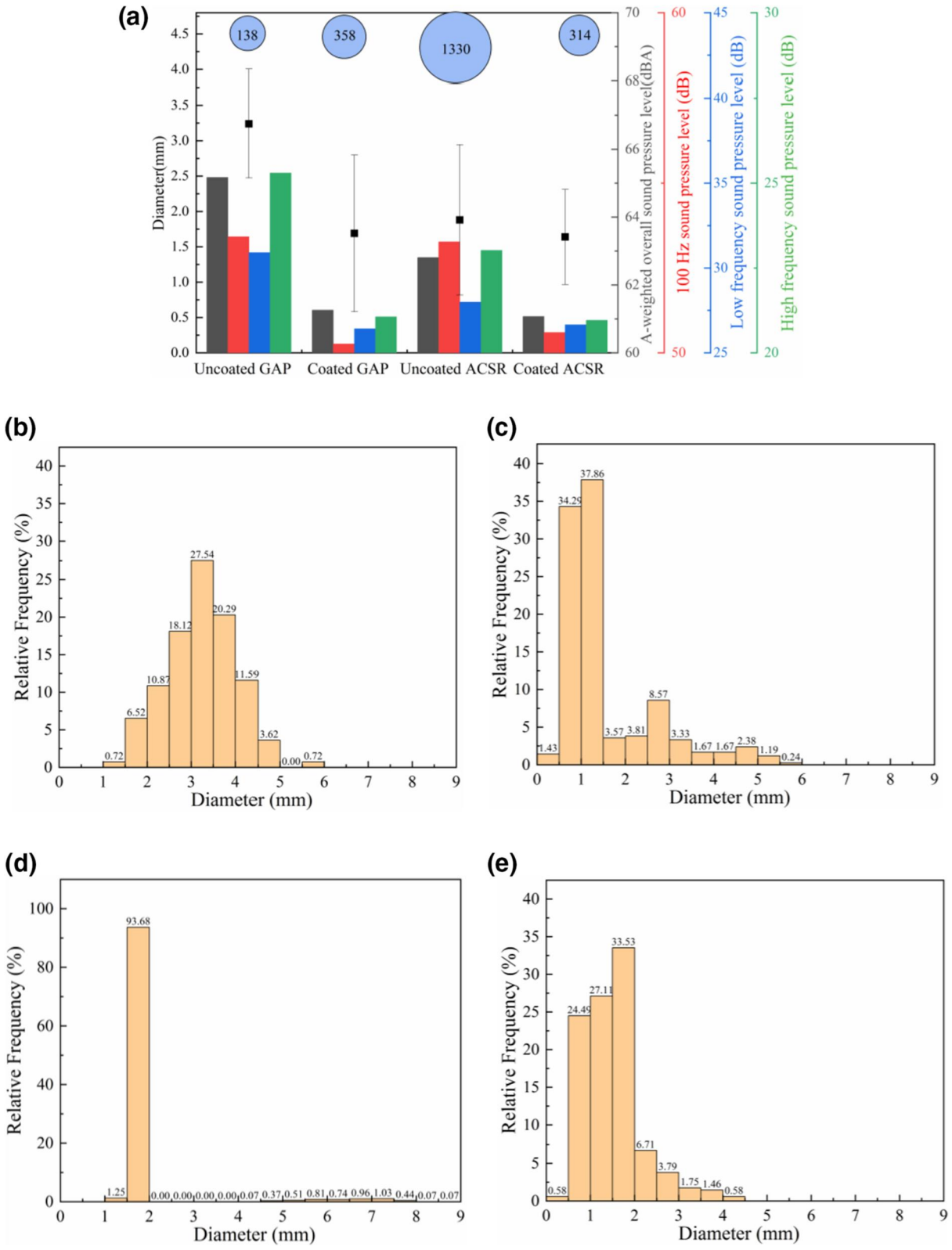

FIGURE 11 (a) The surface drop size distribution on GAP and ACSR conductors. The central dot represents the mean diameter, the whiskers represent the standard deviation, the circles on the top represent the number of drops and the grey, red, blue and blue bars give the A-weighted overall sound pressure level, 100 Hz, low-frequency and high-frequency noise levels, respectively. (b) and (c) show drop size histograms on uncoated and coated GAP, respectively. (d) and (e) show drop size histograms on uncoated and coated ACSR, respectively. All data are at an electric field strength of 21 kV/cm

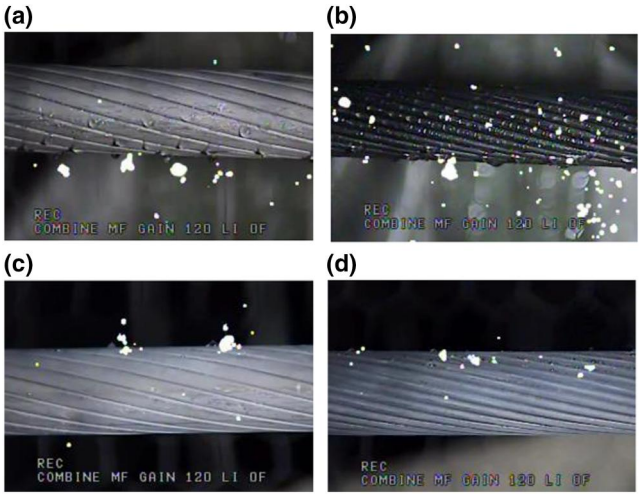

FIGURE 12 The images captured by the UV camera of uncoated and coated conductors at the corona discharge inception voltage. (a) (b) uncoated conductors, (c) (d) coated conductors

The partial discharge magnitude per cycle is analysed by MPD software and plotted in Figure 13. The results show that the PD magnitude per cycle of the coated conductors is lower than uncoated conductors when the electric field is above 14 kV/cm, which correlates to the A-weighted overall sound pressure. The maximum PD magnitude reduction is found at the maximum electric field. The weaker corona discharge associated with the superhydrophobic coating may also be a factor driving the noise reduction.

4 | DISCUSSION

Both coated conductors show lower noise levels at 100 Hz, low frequency and high frequency, and A-weighted overall sound pressure level than uncoated ones. This is consistent with Miyajima and Tanabe's A-weighted sound pressure measurements [35]. The 100 Hz noise level shows a drop at 11 kV/cm, seen in Figure 7. Figure 9 shows that this electric field is the threshold value to trigger droplets vibration and ejection. The droplet size distributions on coated conductors at 10 kV/cm and 11 kV/cm show that the average diameter of droplets on the coated GAP conductor decreases from 2.28 to 1.93 mm with the falling droplets number from 121 to 95. A similar trend is also seen on the coated ACSR conductor—the decreasing mean diameter and number from 2.01 to 1.57 mm and 103 to 93, respectively.

Fewer and smaller droplets remain, likely accounting for the minimum in 100 Hz noise level at 11 kV/cm.

The correlation of droplets size distribution to noise levels suggests that the size of drops retained on a conductor is an important factor in driving 100 Hz noise level and A-weighted overall sound pressure levels. The number of drops is not strongly correlated with noise levels possibly due to the inclusion of many small drop sizes in the count. It therefore appears that the presence of the coating on a conductor reduces the average drop size but can increase the number of

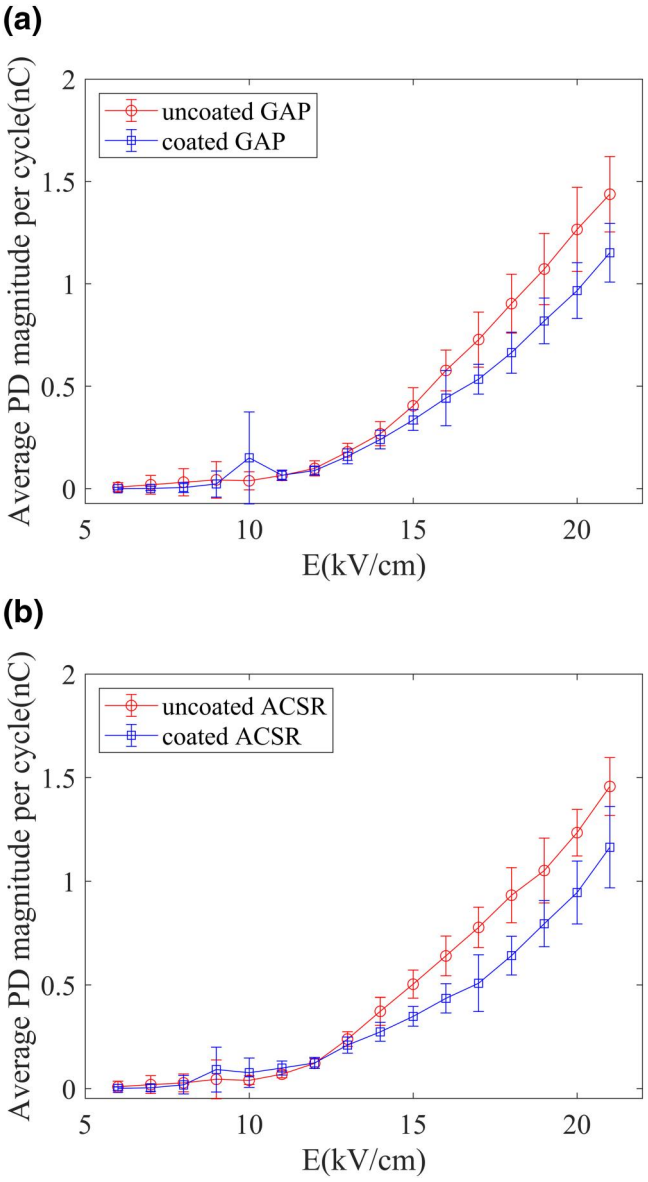

FIGURE 13 The average partial discharge magnitude per cycle of uncoated and coated conductors (a) GAP, (b) ACSR

droplets on the conductor surface. The fewer and smaller droplets result in the higher corona discharge inception voltage and lower PD magnitude. The overall effect is a reduction in noise level on a coated conductor. The different strand geometries of ACSR and GAP result in the various droplets distribution shown in Figure 11. The round strands of ACSR may trap smaller droplets than GAP with flat strands.

The pendant and sessile droplets on the conductor behave differently under AC voltage [23], which may be another factor influencing the noise output. The mean diameter and number of the pendant and sessile droplets on conductors are shown in Table 3. For uncoated conductors, the pendant droplets are dominant and sessile droplets are more prevalent on coated conductors. The pendant droplets are mostly larger and fewer than sessile droplets. The pendant droplets under the overhead line conductors will increase the

TABLE 3 The number and size distribution of pendant and sessile drops on conductors

	Pendant drop		Sessile drop	
	Mean diameter (mm)	**Number**	**Mean diameter (mm)**	**Number**
Uncoated GAP	3.81	27	–	0
Coated GAP	2.86	6	2.76	98
Uncoated ACSR	6.65	40	1.67	202
Coated ACSR	–	0	2.05	56

electric field [33]. Compared with a sessile droplet, a pendant droplet will discharge at a lower voltage [48]. According to Straumann [18], 100 Hz noise is emitted by the ions drift during discharge. The harmonic components of audible noise were proven to be related to corona current [20]. Therefore, the change from big pendant droplets to small sessile droplets on a coated conductor may result in less corona discharge and that may be another reason for the reductions in audible noise output. Further measurements including partial discharge testing for sessile and pendant drop may provide further insight into this result.

5 | CONCLUSIONS

A semi-anechoic chamber was used to measure sound produced by two designs of overhead line samples at high voltages during precipitation, to compare the noise-reducing benefits of a superhydrophobic coating. Noise output at all frequencies was observed to increase above background levels as electric field strength increased. The superhydrophobic coating generally reduced audible noise at low (<1000 Hz) and high (>1000 Hz) frequencies and also A-weighted overall sound pressure level was reduced, especially when the electric field is above 14 kV/cm. Sound pressure levels at 100 Hz show the largest relative reduction at 11 kV/cm when coated with superhydrophobic material, which was attributed to the onset of drop vibration and droplet ejection, reducing the relative presence of drops on the conductor surface. The coating reduced sound output (power) by approximately 33%–44% on both conductor types, equating to an estimated psychoacoustic perceived loudness reduction of approximately 13%–23%. The corona discharge magnitude is also reduced with the superhydrophobic coating. Examining the droplet size distribution and the number of drops on coated conductors, it appears likely that a reduction in the number of large droplets and the change from pendant droplets to sessile droplets drive the decrease in the noise level.

ACKNOWLEDGMENTS

This work is supported in part by Chinese Scholarship Council and The University of Manchester.

DATA AVAILABILITY STATEMENT

The data that support the findings of this study are available from the corresponding author upon reasonable request.

ORCID

Xu Zhang https://orcid.org/0000-0002-8772-5826

REFERENCES

1. Huang, D., et al.: Ultra high voltage transmission in China: developments, current status and future prospects. Proc. IEEE. 97(3), 555–583 (2009)
2. Dunlop, R.D., Gutman, R., Marchenko, P.P.: Analytical development of loadability characteristics for EHV and UHV transmission lines. IEEE Trans. Power Apparatus Syst. PAS-98(2), 606–617 (1979)
3. Chamia, M., Liberman, S.: Ultra high speed relay for EHV/UHV transmission lines — development, design and application. IEEE Trans. Power Apparatus Syst. PAS-97(6), 2104–2116 (1978)
4. Scherer, H.N., Vassell, G.S.: Transmission of electric power at Ultra-High Voltages: current status and future prospects. Proc. IEEE. 73(8), 1252–1278 (1985)
5. Hedtke, S., Bleuler, P., Franck, C.M.: Outdoor investigation of the corona characteristics and audible noise of a hybrid AC/DC overhead line. IEEE Trans. Power Deliv. 36(6), 3309–3317 (2021)
6. Hedtke, S., et al.: HVDC corona current characteristics and audible noise during wet weather transitions. IEEE Trans. Power Deliv. 35(2), 1038–1046 (2020)
7. Pischler, O., Schichler, U.: Influence of hydrophilic conductor surface treatments on OHL audible noise. Proc. Int. Conf. Properties and Applications of Dielectric Materials, Xi'an, China, pp. 78-81. (2018)
8. Xu, P., et al.: HVAC corona current characteristics and audible noise during rain. IEEE Trans. Power Deliv. 36(1), 331–338 (2021)
9. Straumann, U., Fan, J.: Tonal component of the audible noise from Uhv-Ac transmission lines. Proc. ISH., Cape, Town, August, pp. 1-5. (2009)
10. Engel, Z., Wszolłek, T.: Audible noise of transmission lines caused by the corona effect: analysis, modelling, prediction. Appl. Acoust. 47(2), 149–163 (1996)
11. He, W., et al.: Audible noise spectral characteristics of high-voltage ac bundled conductors at high altitude. IET Gener. Transm. Distrib. 15(8), 1304–1313 (2021)
12. Zhang, X., et al.: Acoustic noise emitted from overhead line conductors with superhydrophobic coating. Proc. Int. Electrical Insulation Conference, Calgary, Canada, pp. 87–90. (2019)
13. He, W., et al.: Investigation of audible noise performance of HVAC conductor bundles at altitude of 2261 m. CSEE J. Power Energy Syst. (2020). https://doi.org/10.17775/CSEEJPES.2020.02970
14. Chang, J.S., Lawless, P.A., Yamamoto, T.: Corona discharge processes. IEEE Trans. Plasma Sci. 19(6), 1152–1166 (1991)
15. Carberry, R.E., et al.: Measurement of audible noise from transmission lines. IEEE Trans. Power Apparatus Syst. PAS-100(3), 1440–1452 (1981)
16. Piercy, J.E., Embleton, T.F.W., Sutherland, L.C.: Review of noise propagation in the atmosphere. J. Acoust. Soc. Am. 61(6), 1403–1418 (1977)
17. Waye, K.P.: Effects of low frequency noise on sleep. Noise Health. 6(23), 87–91 (2004)
18. Straumann, U.: Mechanism of the tonal emission from ac high voltage overhead transmission lines. J. Phys. D Appl. Phys. 44(7), 1–9 (2011)

19. Straumann, U.: Simulation of the space charge near coronating conductors of ac overhead transmission lines. J. Phys. D Appl. Phys. 44(7), 1–9 (2011)
20. Li, X., et al.: Correlation between audible noise and corona current generated by AC corona discharge in time and frequency domains. Phys. Plasmas. 25(6), 1–14 (2018)
21. Li, X., et al.: Statistical analysis of audible noise generated by AC corona discharge from single corona sources. High Volt. 3(3), 207–216 (2018)
22. Teich, T.H., Weber, H.J.: Origin and abatement of tonal emission from high voltage transmission lines. Elektrotech. Inftech. 119(1), 22–27 (2002)
23. Li, Q., et al.: The impact of water droplet vibration on corona inception on conductors under 50 Hz AC fields. IEEE Trans. Power Deliv. 33(5), 2428–2436 (2018)
24. Fujii, O., et al.: Vibration of a water droplet on a polymeric insulating material subjected to AC voltage stress. IEEE Trans. Dielectr. Electr. Insul. 17(2), 566–571 (2010)
25. Fujii, O., et al.: A basic study on the effect of voltage stress on a water droplet on a silicone rubber surface. IEEE Trans. Dielectr. Electr. Insul. 16(1), 116–122 (2009)
26. Bian, X., et al.: Influence of aged conductor surface conditions on AC corona-generated audible noise with a corona cage. IEEE Trans. Dielectr. Electr. Insul. 18(3), 809–818 (2011)
27. Chen, L., et al.: Comparison of methods for determining corona inception voltages of transmission line conductors. J. Electrost. 71(3), 269–275 (2013)
28. Zhu, J., et al.: Experimental studies on effects of surface morphologies on corona characteristics of conductors subjected to positive DC voltages. High Volt. 5(4), 489–497 (2020)
29. Zhu, J., et al.: Dynamics and concentration variations of fine particles of different sizes in the vicinity of DC conductors. Appl. Phys. Lett. 117(14), 1–7 (2020)
30. Ianna, F., Wilson, G.L., Bosack, D.J.: Spectral characteristics of acoustic noise from metallic protrusions and water droplets in high electric fields. IEEE Trans. Power Apparatus Syst. PAS-93(6), 1787–1796 (1974)
31. Comber, M.G., Nigbor, R.J.: Audible noise performance of regular and asymmetric bundles and effect of conductor aging on project UHV's three-phase test line. IEEE Trans. Power Apparatus Syst. PAS-98(2), 561–572 (1979)
32. Brown, M.T., Rebbapragada, R.V., Dorazio, T.F.: Utility system demonstration of six phase power transmission. Proc. Int. Conf. Power Engineering Society Transmission and Distribution, Dallas, USA, pp. 983–999. (1991)
33. Tanabe, K., Takebe, T., Isozaki, M.: Reduction of audible noise using asymmetrical bundles for 1000 kV transmission lines: full-scale test results of Akagi test line. IEEE Trans. Power Deliv. 11(3), 1482–1491 (1996)
34. Héroux, P., Maruvada, P.S., Trinh, N.G.: High voltage AC transmission lines: reduction of corona under foul weather. IEEE Trans. Power Apparatus Syst. PAS-101(9), 3009–3017 (1982)
35. Miyajima, K., Tanabe, K.: Evaluation of audible noise from surface processing conductors for AC overhead transmission line. Electr. Eng. Jpn. 159(3), 19–25 (2007)
36. Song, D., Song, B.W., Hu, H.B.: The analysis of noises of flows across the superhydrophobic surfaces with microscale structures. Adv. Mater. Res. 535–537, 319–322 (2012)
37. Malavasi, I., et al.: Assessing durability of superhydrophobic surfaces. Surf. Innov. 3(1), 49–60 (2015)
38. Lian, C., et al.: Assessing the superhydrophobic performance of laser micropatterned aluminium overhead line conductor material. IEEE Trans. Power Deliv., 1–7 (2021)
39. Lian, C., et al.: Ageing behaviours of superhydrophobic and icephobic coatings on overhead line systems. Proc. Int. Conf. Dielectrics, Valencia, Spain, pp. 138–141. (2020)
40. Wang, D., et al.: Design of robust superhydrophobic surfaces. Nature. 582(7810), 55–5 (2020)
41. Li, Q., et al.: Acoustic noise evaluation for overhead line conductors using an anechoic chamber. IEEE Trans. Power Deliv. 32(4), 1835–1843 (2017)
42. Li, Q.: Acoustic noise emitted from overhead line conductors. Ph.D. thesis, University of Manchester (2013)
43. International Standard IEC 60060: High-voltage testing techniques — Part 1: General definitions and test requirements (1990)
44. Kolcio, N., DiPlacido, J., Dietrich, F.M.: Apple grove 750 KV project-two year statistical analysis of audible noise from conductors at 775 KV and ambient noise data. IEEE Trans. Power Apparatus Syst. 96(2), 560–570 (1977)
45. International Standard 80000-8: Quantities and units — Part 8: Acoustics (2006)
46. Crocker, M.J.: Theory of sound—predictions and measurement. In: Handbook of noise and vibration control, pp. 17–42. John Wiley & Sons, Ltd (2007)
47. Tian, Y., et al.: A combined experimental and numerical study on droplet-impact induced breakup and ejection behaviors in vertical electric field. Chem. Eng. Sci. 239, 1–12 (2021)
48. Swift, D.A.: Flashover of an insulator surface in air due to polluted water droplets. Proc. Int. Conf. Roperties Appl. Dielectr. Mater., Brisbane, Australia, pp. 550–553. (1994)

How to cite this article: Zhang, X., et al.: Experimental verification of the potential of superhydrophobic surfaces in reducing audible noise on HVAC overhead line conductors. High Volt. 7(4), 692–704 (2022). https://doi.org/10.1049/hve2.12200